Computers and Electrical Engineering 37 (2011) 789–797

Contents lists available at ScienceDirect

Computers and Electrical Engineering

journal homepage: www.elsevier.com/locate/compeleceng

Multi-focus image fusion for visual sensor networks in DCT domain ☆

Mohammad Bagher Akbari Haghighat [a], Ali Aghagolzadeh [a,b,*], Hadi Seyedarabi [a]

[a] Faculty of Electrical and Computer Engineering, University of Tabriz, Tabriz, Iran
[b] Faculty of Electrical and Computer Engineering, Babol University of Technology, Babol, Iran

ARTICLE INFO

Article history:
Available online 25 May 2011

ABSTRACT

The objective of image fusion is to combine relevant information from multiple images into a single image. The discrete cosine transform (DCT) based methods of image fusion are more efficient and time-saving in real-time systems using DCT based standards of still image or video. Existing DCT based methods are suffering from some undesirable side effects like blurring or blocking artifacts which reduce the quality of the output image. Furthermore, some of these methods are rather complex and this contradicts the concept of the simplicity of DCT based algorithms. In this paper, an efficient approach for fusion of multi-focus images based on variance calculated in DCT domain is presented. Due to simplicity of our proposed method, it can be easily used in real-time applications. The experimental results verify the efficiency improvement of our method both in output quality and complexity reduction in comparison with several recent proposed techniques.

1. Introduction

In all sensor networks, every sensor can observe environment, produce and transfer data. Visual sensor networks (VSN) is the term used in the literature to refer to a system with a large number of cameras geographically spread at monitoring points [1]. In VSN, sensors are cameras which can record either still images or video sequences. Therefore, the processing of output information is related to image processing and machine vision subjects.

A distinguished feature of visual sensors or cameras is the great amount of generated data. This characteristic requires more local processing resources to deliver only the useful information represented in a conceptualized level [2]. Image fusion is generally defined as the process of combining multiple source images into a smaller set of images, usually a single one, which contains a more accurate description of the scene than any of the individual source images. The goal of image fusion, besides reducing the amount of data in network transmissions, is to create new images that are more informative and suitable for both visual perception and further computer processing [3].

Due to the limited depth of focus in optical lenses, only the objects at a particular depth in the scene are in focus and those in front of or behind the focus plane will be blurred. In VSN we have the opportunity of extending the depth of focuses using multiple cameras.

So far, several researches have been focused on image fusion which are performed on the images in the spatial domain [4–8]. The algorithms based on multi-scale decompositions are more popular. The basic idea is to perform a multi-scale transform on each source image, and then integrate all of these decomposition coefficients to produce a composite representation. These methods combine the source images by monitoring a quantity that is called the activity level measure. The activity level determines the quality of each source image. The integration can be carried out either by choosing the coefficients with larger activity level or a weighted average of the coefficients. The fused image is finally reconstructed by

☆ Reviews processed and approved for publication to Dr. Ferat Sahin.

* Corresponding author at: Faculty of Electrical and Computer Engineering, University of Tabriz, Tabriz, Iran. Tel.: +984113393720; fax: +984113300829.
E-mail addresses: haghighat87@ms.tabrizu.ac.ir (M.B.A. Haghighat), aghagol@tabrizu.ac.ir (A. Aghagolzadeh), seyedarabi@tabrizu.ac.ir (H. Seyedarabi).

0045-7906/$ - see front matter © 2011 Published by Elsevier Ltd.
doi:10.1016/j.compeleceng.2011.04.016

performing the inverse multi-scale transform. Examples of this approach include Laplacian, gradient, morphological pyramids, and the superior ones, discrete wavelet transform (DWT) [9] and shift invariant discrete wavelet transform (SIDWT) [10]. The two later methods are treated as standard methods for image fusion in the literature. A professional survey on these methods may be found in [11,12].

In general, most of the spatial domain image fusion methods are complex and time-consuming which are not suitable to be performed on real-time applications. In VSN, especially when the links between nodes are wireless, the consumed energy for data processing is much less than the consumed energy for communication. Therefore, in most of the sensor network systems, data are compressed before transmission to the other nodes. In VSN, images are compressed in camera nodes and then transmitted to the fusion agent, and afterwards, the compressed fused image will be saved or transmitted to an upper node. Hence, when the source images are coded in Joint Photographic Experts Group (JPEG) standard, as a prevalent standard, or when the fused image will be saved or transmitted in JPEG format, the fusion methods which are applied in DCT domain will be more efficient.

We denote A and B as the output images of two cameras that have been compressed in JPEG coding standard in the sensor agent and transmitted to the fusion agent of VSN. In the case of using the spatial domain fusion methods, these images must initially be decoded and transferred into the spatial domain. Then, after applying the fusion procedure, the fused image must be encoded again in order to be stored or transmitted to an upper node. But in case of using a DCT based approach, there is no need for these complex decoding and encoding procedures.

Recently, Tang [13] has considered the above mentioned issue of complexity reduction and proposed two image fusion techniques in DCT domain, namely, DCT + Average and DCT + Contrast. Tang has implemented his proposed methods on 8×8 DCT blocks defined in JPEG standard. DCT + Average obtains the DCT representation of the fused image by simply taking the average of all the DCT coefficients of all the input images. This simple method of averaging leads to some undesirable side effects including blurring.

For the second technique called DCT + Contrast, fusion criterion or activity level is based on a contrast measure which is calculated for every 63 AC coefficients of the blocks from source images. Then the contrast measures of each coefficient in the corresponding blocks in source images are compared and the coefficient with the highest activity level is selected. The DCT block of the output image is made up of AC coefficients with the highest contrast measures selected by comparing procedure, and DC coefficient of each block in the output image is the average of DC coefficients of the corresponding blocks in the input images. This algorithm is also complex in calculating the contrast measure for each coefficient. Furthermore, it suffers from some side effects including blocking artifacts due to the manipulation in the diverse selection of DCT coefficients.

In order to reduce the complication for the real-time applications and also enhance the quality of the output image, an image fusion technique in DCT domain is proposed in this paper. Here, the variance of 8×8 DCT coefficients in a block is considered as a contrast criterion to be used for activity level measure. Then, a consistency verification (CV) stage increases the quality of the output image. Simulation results and comparisons show the considerable improvement in the quality of the output image and reduction in computation complexity.

This paper is organized as follows: in Section 2, the basic concepts of our approach are discussed which is based on variance calculation in DCT domain. Section 3 presents our proposed method of image fusion. In Section 4 the simulation results are demonstrated and analyzed; and finally the main conclusion is drawn in Section 5.

2. DCT block analysis

2.1. DCT in compression standards

Several commercial standards widely used in image and video compression are based on DCT. Some examples include JPEG still image coding standard [14], Motion-JPEG, MPEG and the ITU H26X video coding standards [15].

In JPEG encoder, the given image is first partitioned into nonoverlapping 8×8 blocks. The 8-bit pixels of an image are in the range of 0:255, so the coding process begins with a "Level Shifting" stage. In order to reduce the amount of DC coefficient, the input data is shifted to the range -128:127, so that it becomes distributed about zero. The two-dimensional DCT is then performed on each 8×8 block. Afterwards, DCT coefficients in every block are quantized using a specified quantization table. In the step of quantization, a large number of small coefficients (usually high frequency components) are quantized to zeros which makes the quantization a lossy process. The 8×8 blocks of quantized coefficients are then rearranged in a zigzag order so that the high frequency coefficients with zero values are grouped together at the end of the rearranged array. Next, run-level procedure and Huffman encoder are used to encode the coefficients. In the decoder side, each block of the compressed data is decoded and then dequantized (reconstructed) by using quantization table. Finally, the reconstructed coefficients are transformed back into an image block by inverse DCT.

2.2. Variance in DCT domain as a contrast criterion

Two-dimensional DCT transform of an $N \times N$ block of an image $x(m, n)$ is defined as:

$$d(k,l) = \frac{2\alpha(k)\alpha(l)}{N} \times \sum_{m=0}^{N-1} \sum_{n=0}^{N-1} x(m,n) \times \cos\left[\frac{(2m+1)\pi k}{2N}\right] \times \cos\left[\frac{(2n+1)\pi k}{2N}\right] \quad (1)$$

where $k, l = 0, 1, \ldots, N-1$ and

$$\alpha(k) = \begin{cases} \frac{1}{\sqrt{2}}, & \text{if } k = 0 \\ 1, & \text{otherwise} \end{cases} \tag{2}$$

The inverse DCT (IDCT) is also defined as:

$$x(m,n) = \sum_{k=0}^{N-1}\sum_{l=0}^{N-1} \frac{2\alpha(k)\alpha(l)}{N} \times d(k,l) \times \cos\left[\frac{(2m+1)\pi k}{2N}\right] \times \cos\left[\frac{(2n+1)\pi k}{2N}\right] \tag{3}$$

where $m, n = 0, 1, \ldots, N-1$.

In (1), $d(0,0)$ is the DC coefficient and the other $d(k,l)$'s are the AC coefficients of the block. The normalized transform coefficients $\hat{d}(k,l)$'s are defined as below:

$$\hat{d}(k,l) = \frac{d(k,l)}{N} \tag{4}$$

Mean value, μ, and variance, σ^2, of an $N \times N$ block in the spatial domain are calculated as:

$$\mu = \frac{1}{N^2}\sum_{m=0}^{N-1}\sum_{n=0}^{N-1} x(m,n) \tag{5}$$

$$\sigma^2 = \frac{1}{N^2}\sum_{m=0}^{N-1}\sum_{n=0}^{N-1} x^2(m,n) - \mu^2 \tag{6}$$

As we know the mean value, μ, of the $N \times N$ block is given by $\hat{d}(0,0)$. With a little mathematical calculation, we can also provide the variance of the block from DCT coefficients. We have:

$$\begin{aligned} \sum_{m=0}^{N-1}\sum_{n=0}^{N-1} x^2(m,n) &= \sum_{m=0}^{N-1}\sum_{n=0}^{N-1} x(m,n)\cdot x(m,n) \\ &= \sum_{m=0}^{N-1}\sum_{n=0}^{N-1} x(m,n) \times \left(\sum_{k=0}^{N-1}\sum_{l=0}^{N-1} \frac{2\alpha(k)\alpha(l)}{N}\cdot d(k,l)\cdot \cos\left[\frac{(2m+1)\pi k}{2N}\right]\cdot \cos\left[\frac{(2n+1)\pi k}{2N}\right]\right) \end{aligned}$$

By interchanging the positions of the summations, we will have:

$$\begin{aligned} &= \sum_{k=0}^{N-1}\sum_{l=0}^{N-1} \frac{2\alpha(k)\alpha(l)}{N} \times d(k,l) \times \sum_{m=0}^{N-1}\sum_{n=0}^{N-1} x(m,n) \times \cos\left[\frac{(2m+1)\pi k}{2N}\right] \times \cos\left[\frac{(2n+1)\pi k}{2N}\right] \\ &= \sum_{k=0}^{N-1}\sum_{l=0}^{N-1} \frac{2\alpha(k)\alpha(l)}{N} \times d(k,l) \times \frac{N \times d(k,l)}{2\alpha(k)\alpha(l)} \\ &= \sum_{k=0}^{N-1}\sum_{l=0}^{N-1} d(k,l)\cdot d(k,l) \\ &\Rightarrow \sum_{m=0}^{N-1}\sum_{n=0}^{N-1} x^2(m,n) = \sum_{k=0}^{N-1}\sum_{l=0}^{N-1} d^2(k,l) \end{aligned} \tag{7}$$

Then, from (6) and (7):

$$\begin{aligned} &\sigma^2 = \frac{1}{N^2}\sum_{m=0}^{N-1}\sum_{n=0}^{N-1} x^2(m,n) - \mu^2 \\ &\Rightarrow \sigma^2 = \sum_{k=0}^{N-1}\sum_{l=0}^{N-1} \frac{d^2(k,l)}{N^2} - \hat{d}^2(0,0) \end{aligned} \tag{8}$$

In conclusion, the variance of an $N \times N$ block of pixels can be exactly calculated from its DCT coefficients by sum of the squared normalized AC coefficient of the DCT block.

3. Proposed method: variance based image fusion in DCT domain

In multi-focus images, the focused area is more informative. This information is behind the clear details of that region which is corresponding to the high variance. Variance value is usually assumed as a contrast measure in image processing applications. It was shown in Section 2 that the calculation of the variance value in DCT domain is very easy. Therefore, we can use the variance value as the activity level measure of the 8×8 blocks of the source images.

Fig. 1 illustrates the general framework of a JPEG encoder combining with image fusion for VSN. Here, for simplicity, we consider the processing of just two source images *A* and *B*, but the algorithm can be extended straightforwardly for more than two source images. Moreover, it is assumed that the source images are previously aligned with some registration methods.

As Fig. 1 shows, after dividing the source images into blocks of 8×8 pixels and calculating the DCT coefficients for each block, the fusion algorithm is performed. Here the variance values of the corresponding blocks from source images are calculated by (8) as the activity level measures. Then, the block with the highest activity level is selected as the appropriate one for the fused image. Finally, the DCT presentation of the fused image is made up of blocks with the larger variances that are from source image either *A* or *B*.

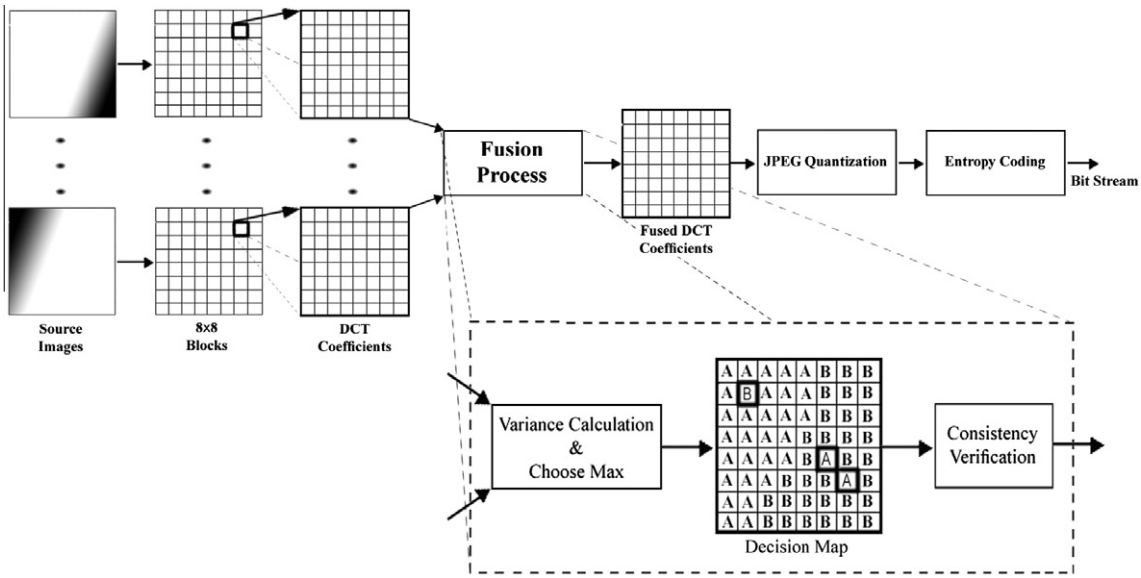

Fig. 1. A general framework of a JPEG encoder combining with proposed image fusion method.

Fig. 2. Images used for simulations.

3.1. Consistency verification (CV)

Assume a region in a scene including several blocks that is completely in the depth of focus of image *A*. Following the above mentioned process, all the blocks in this region must be chosen from image *A*. However, there can be some errors due to noise or undesired effects during the selection process that can lead to erroneous selection of some blocks from image *B*. This defect can be solved with a consistency verification procedure. The incorrect decision map is demonstrated in Fig. 1.

Li et al. [9] introduced a majority filter that can be utilized in consistency verification. If the center block comes from source image *B* while the majority of the surrounding blocks come from source image *A*, the center sample is simply switched to the corresponding block in source image *A*. The fused image is finally obtained based on this modified decision map.

Here, consistency verification is applied in a 3×3 neighborhood window. If the window size increases, the quality of the output image will obviously raise at the expense of complexity increase. It should be mentioned that our experiments show that instead of using a 5×5 window and considering 24 items, using a 3×3 window for two consequential times and considering only 16 items in total, will be more efficient in both quality and complexity.

Table 1
Average SSIM values of algorithms.

DCT + Average	DCT + Contrast	DWT	SIDWT	DCT + Variance (proposed)	DCT + Variance + CV (proposed)
0.90787	0.94672	0.98112	0.98389	0.97654	0.99872

Table 2
Average run-time values of algorithms (in microseconds per 8×8 block).

DCT + Average	DCT + Contrast	DCT + Variance (proposed)	DCT + Variance + CV (proposed)
11.39323	264.35004	16.14041	64.56163

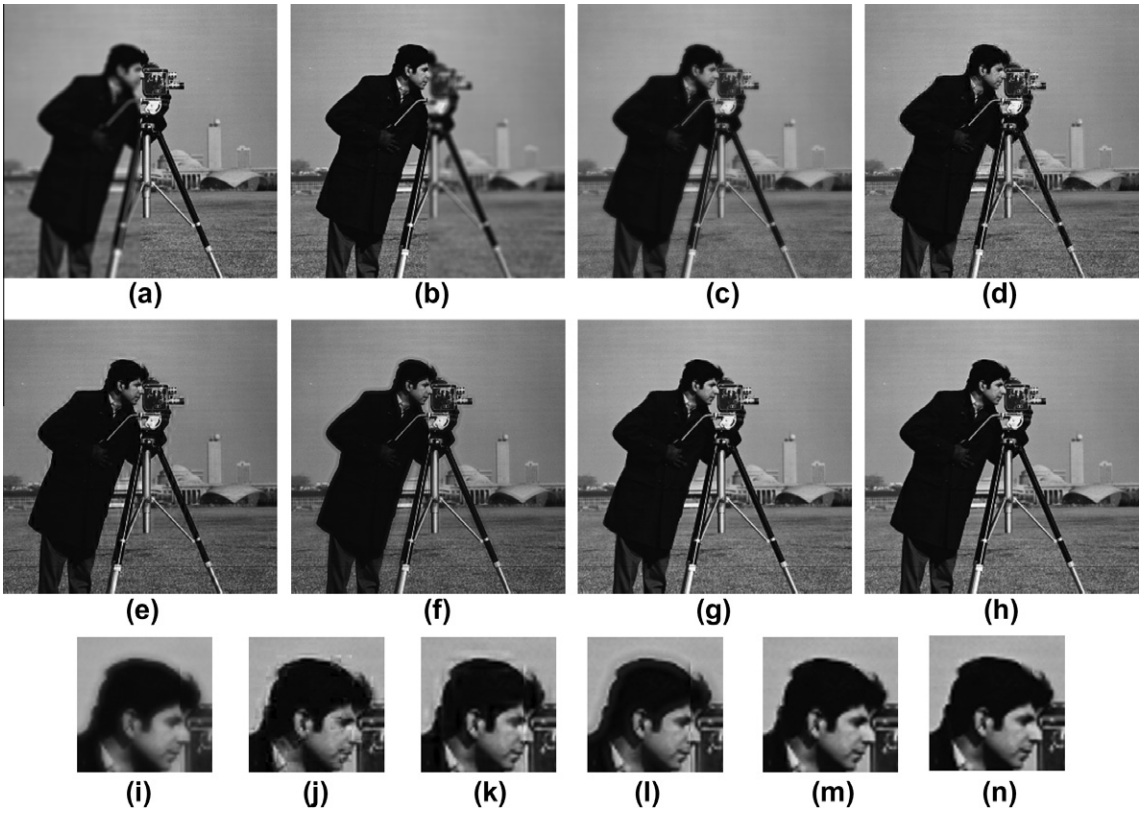

Fig. 3. Source images "Cameraman" and the fusion results. (a) The first source image with focus on the right. (b) The second source image with focus on the left. (c) DCT + Average result. (d) DCT + Contrast result. (e) DWT result. (f) SIDWT result. (g) Result of the proposed DCT + Variance algorithm. (h) Result of the proposed algorithm with consistency verification DCT + Variance + CV. (i), (j), (k), (l), (m), (n) are the local magnified version of (c), (d), (e), (f), (g) and (h), respectively.

4. Experimental results and analysis

In this section, experimental results of the presented image fusion method are given and evaluated by comparing with the results obtained by four other prominent techniques. Two of them are DCT based image fusion techniques, namely, DCT + Average and DCT + Contrast proposed in [13], and the other two techniques are standard wavelet based fusion (DWT) [9] and the shift invariant wavelet based technique (SIDWT) [10] that have been briefly described in Section 1.

4.1. Performance measure

Although there have been many attempts, no universally accepted criterion has emerged yet for objectively evaluating image fusion performance. This problem partially lies in the difficulty of defining an ideal fused image. Besides the subjective evaluation, in order to have a quantitative comparison of the fusion methods, we adopt the quality measure proposed by Li et al. [9]. Here the out-of-focus images are artificially created by low-pass filtering of some areas in an ideal image. The structural similarity measure (SSIM) [16], as a well-known quality criterion, is used for objective evaluation in this section.

On the other hand, in real applications, it is difficult to have an ideal image which is focused in all of its parts. Therefore, in order to evaluate our algorithm on real multi-focus images, we will use some state-of-the-art fusion performance metrics such as Piella [17], and Petrovic [18] metrics. Piella metric (Q_W) gives an indication about how much of the salient information contained in each of the source images has been transferred into the fused image [17]. Petrovic metric ($Q^{AB/F}$) measures the relative amount of edge information that is transferred from the source images (A and B) into the fused image (F) [18]. In addition, the run-time of the algorithms, under the same circumstances of simulations, can be considered as a complexity criterion.

4.2. Experimental circumstances

The simulations of the fusion methods were conducted with an Intel Core2Duo P8400, 2.26 GHz, FSB 1066 MHz processor. For the wavelet based methods, the DWT with DBSS(2,2) and the SIDWT with Haar basis with three levels of decomposition were considered. For simulation of these two methods, the "Image Fusion Toolbox", kindly provided by Rockinger [19], was used.

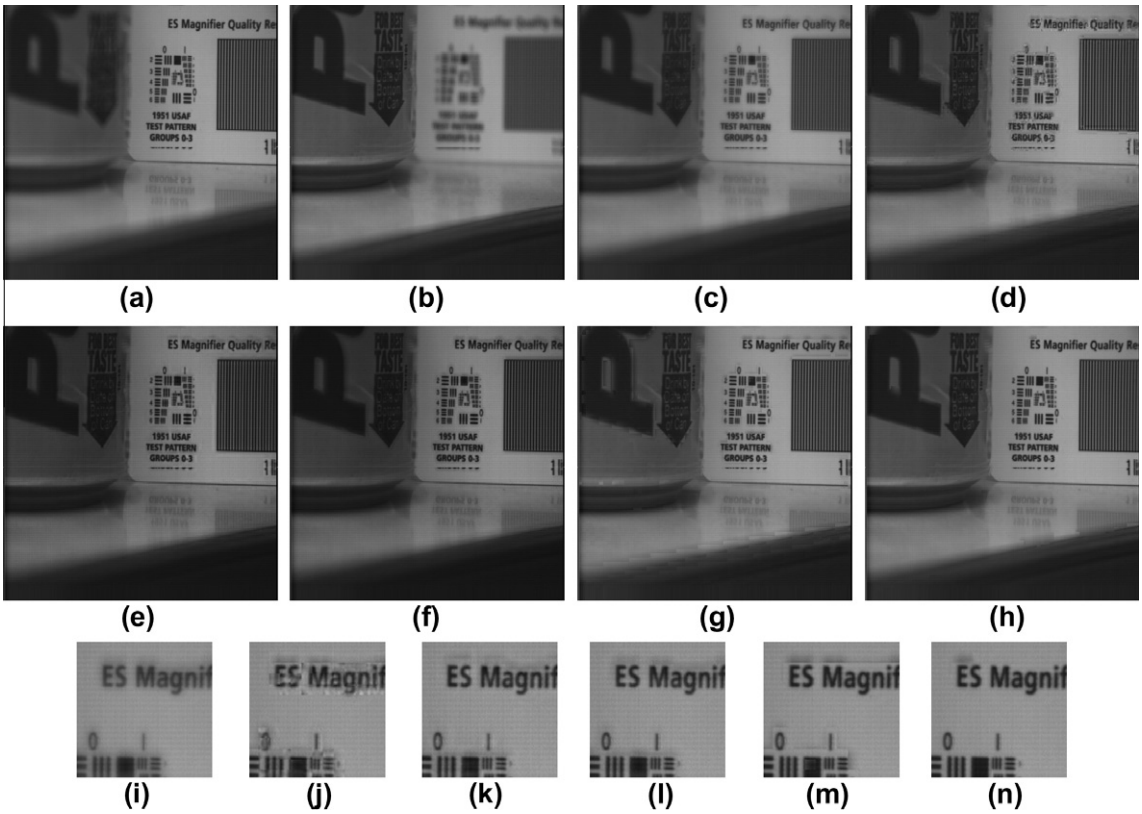

Fig. 4. "Pepsi" database source images and the fusion results: same order as in Fig 3.

4.3. Fusion results evaluation

Initially, the algorithms were performed on eighteen couples of artificially created source images by blurring six standard original images shown in Fig. 2, with three disks of different radiuses 5, 7 and 9 pixels. The images are balanced in the sense that the blurring occurs at both the left and the right halves of the images. The average SSIM values of 18 experimental images are given in Table 1. The first two columns are the average SSIM values of the DCT based algorithms proposed by Tang [13]. The third and fourth columns are corresponding to DWT and SIDWT techniques proposed in [9,10], respectively. The fifth column titled "DCT + Variance" is related to our proposed algorithm without consistency verification and finally the last column demonstrates the average SSIM value of our proposed algorithm after applying consistency verification (CV) in a 3×3 neighborhood which has the most value of SSIM.

The average period of the run-time for reconstruction of every 8×8 block of images in the DCT based methods are given in Table 2. As mentioned before, the DCT based algorithms are considerably faster and less computationally expensive than the other techniques when the images to be fused are saved in JPEG format or when the fused image is saved or transmitted in JPEG format.

From the average SSIM values given in Table 1, it can be clearly seen that the proposed algorithm even without CV is more efficient than the other DCT based algorithms. In addition, after applying CV, there is a considerable improvement in quality, even outperforming the wavelet based algorithms, at the expense of a little complexity. Moreover, the average run-time values given in Table 2, demonstrate the simplicity of our proposed algorithm even after applying CV which results in a noticeable quality improvement.

The subjective test of the resultant images approves the objective measures. Due to the lack of space in this paper, the resultant images of only one test image set is shown in Fig. 3. By carefully observing the fusion results, it is concluded that the method DCT + Average results in the side effect of reduction in contrast or blurring the fused image (Fig. 3c). The method DCT + Contrast results in blocking artifacts (Fig. 3d). In addition there are some artifacts for the wavelet based methods DWT and SIDWT, given in Fig. 3e and f, respectively.

As it can be seen in the magnified images corresponding to DWT and SIDWT, respectively, in Fig. 3k and l, the wavelet based algorithms suffer from a kind of ringing artifact. This ringing artifact is a common problem in wavelet based algorithms. This is due to its finite number of basis functions and using high-pass filter embedded in the details branch of the wavelet tree. In the standard wavelet decomposition, the down-sampling process enlarges the region of ringing effect.

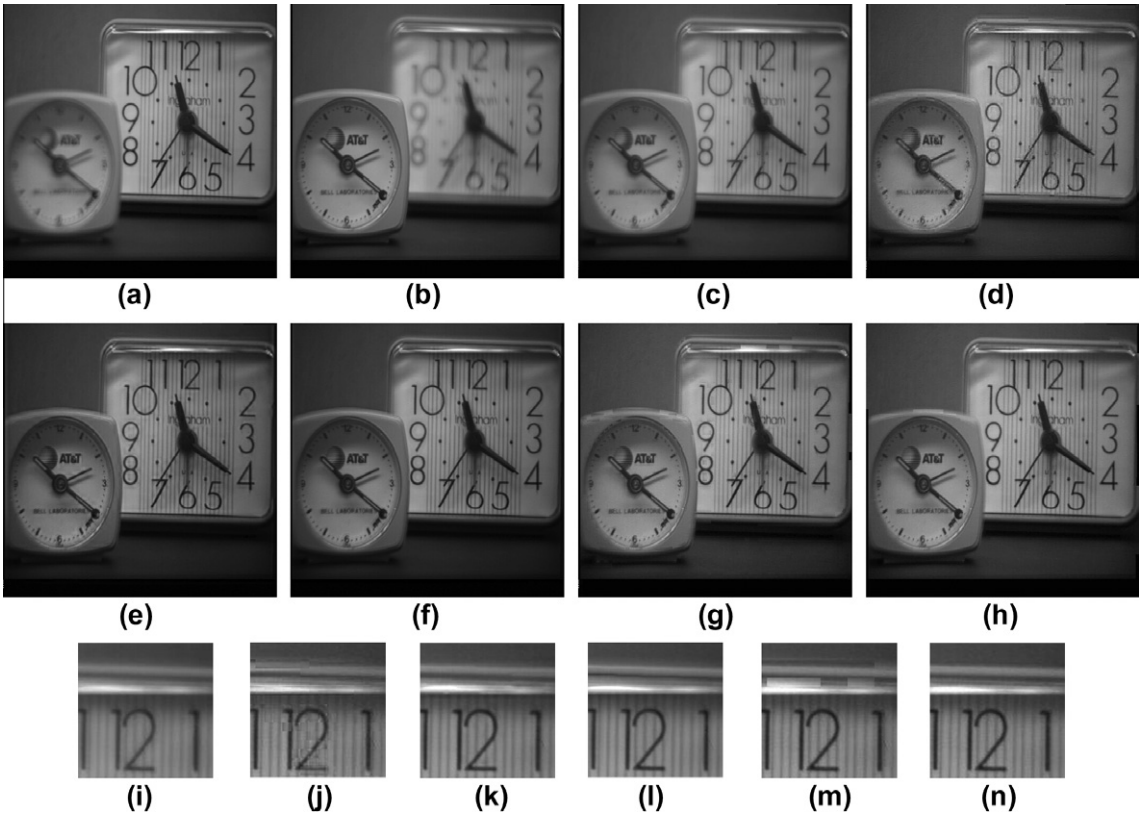

Fig. 5. "Clock" database source images and the fusion results: same order as in Fig 3.

Fig. 3g and h are the results of our proposed method without CV and after applying CV, respectively. It is clearly seen from the images that our proposed algorithm has a considerable improvement in fused image quality.

In order to have some real application experiments, other experiments were conducted on two other well-known images "Pepsi" and "Clock" from Rockinger's database [19] and on "Book" database as a 1280×960 high definition camera image.

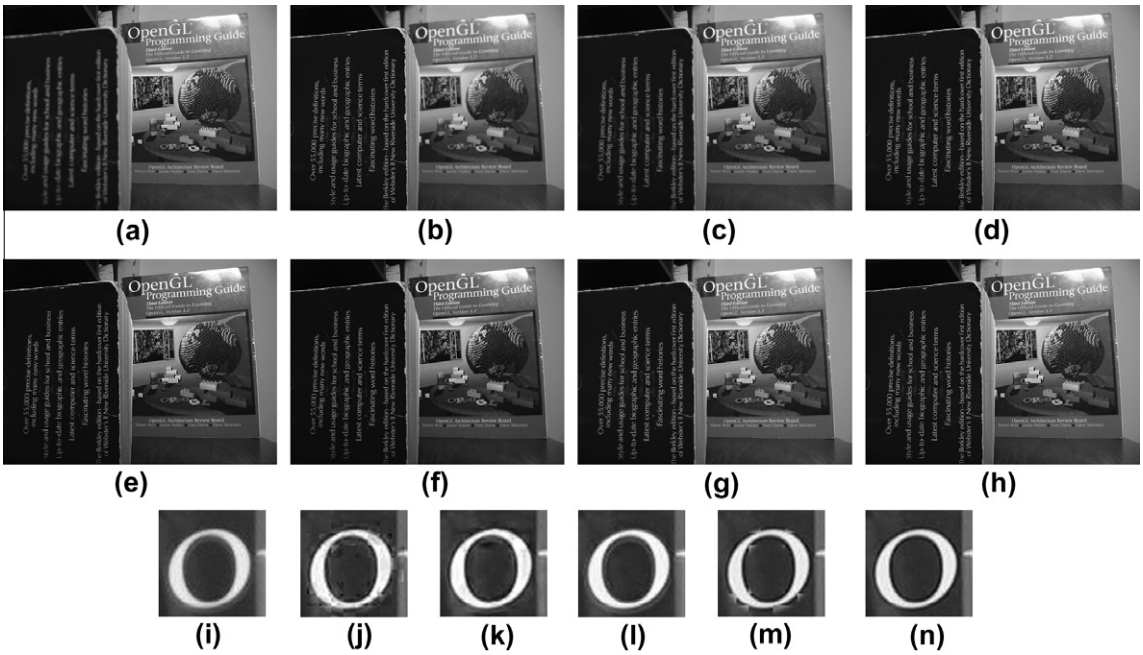

Fig. 6. "Book" database source images and the fusion results: same order as in Fig 3.

Table 3
Objective evaluation of the image fusion algorithms for "Pepsi" database in Fig. 4.

Metric	Method					
	DCT + Average	DCT + Contrast	DWT	SIDWT	DCT + Variance (proposed)	DCT + Variance + CV (proposed)
Q_W	0.8545	0.9073	0.9364	0.9449	0.9275	0.9579
$Q^{AB/F}$	0.6431	0.6696	0.7266	0.7506	0.7716	0.7909

Table 4
Objective evaluation of the image fusion algorithms for "Clock" database in Fig. 5.

Metric	Method					
	DCT + Average	DCT + Contrast	DWT	SIDWT	DCT + Variance (proposed)	DCT + Variance + CV (proposed)

Table 5
Objective evaluation of the image fusion algorithms for "Book" database in Fig. 6.

Metric	Method					
	DCT + Average	DCT + Contrast	DWT	SIDWT	DCT + Variance (proposed)	DCT + Variance + CV (proposed)
Q_W	0.8264	0.8832	0.9149	0.9249	0.9106	0.9261
$Q^{AB/F}$	0.4981	0.5929	0.6619	0.6930	0.7204	0.7296

Similar subjective results are obtained in these experiments as shown in Figs. 4–6. Eventually, the corresponding objective results, acquired from Piella and Petrovic metrics, are given in Tables 3–5. These quantitative evaluations certify the subjective results and prove the superiority of our proposed method.

5. Conclusion

In this paper, a new DCT based fusion technique for multi-focus images was proposed. The method is based on the definition of variance in DCT domain. Simplicity of our proposed method makes it appropriate for real-time applications. Furthermore, utilization of variance in the proposed algorithm, as a proper contrast measure in multi-focus images, leads to better quality of the fused image. Numerous experiments on evaluating the fusion performance were conducted and the results show that the proposed method outperforms the previous DCT based methods both in quality and complexity reduction. Moreover, it is more efficient than the other methods when the source images are in JPEG format or the fused image is saved or transmitted in JPEG format, especially in visual sensor networks. A shortcoming of our method without consistency verification is that it is a bit weak on the boundaries between focused and out-of-focus areas which is solved in DCT + Variance + CV method given in this paper.

References

[1] Perez O, Patricio MA, Garcia J, Carbo J, Molina JM. Fusion of surveillance information for visual sensor networks. In: Proceedings of the IEEE ninth international conference on information fusion (ICIF). p. 1–8.
[2] Castanedo F, Garcia J, Patricio MA, Molina JM. Analysis of distributed fusion alternatives in coordinated vision agents. In: Proceedings of the IEEE eleventh international conference on information fusion (ICIF). p. 1–6.
[3] Drajic D, Cvejic N. Adaptive fusion of multimodal surveillance image sequences in visual sensor networks. IEEE Trans Consum Electron 2007;53(4):1456–62.
[4] Lewis JJ, O'Callaghan RJ, Nikolov SG, Bull DR, Canagarajah N. Pixel- and region-based image fusion with complex wavelets. Inform Fusion 2007;8(2):119–30.
[5] Li S, Yang B. Multifocus image fusion using region segmentation and spatial frequency. Image Vis Comput 2008;26(7):971–9.
[6] Xu L, Roux M, Mingyi H, Schmitt F. A new method of image fusion based on redundant wavelet transform. In: Proceedings of the IEEE fifth international conference on visual information engineering. p. 12–7.
[7] Zaveri T, Zaveri M, Shah V, Patel N. A novel region based multifocus image fusion method. In: Proceedings of IEEE international conference on digital image processing (ICDIP). p. 50–4.
[8] Arif MH, Shah SS. Block level multi-focus image fusion using wavelet transform. In: Proceedings of IEEE international conference on signal acquisition and processing (ICSAP). p. 213–6.
[9] Li H, Manjunath B, Mitra S. Multisensor image fusion using the wavelet transform. Graph Models Image Process 1995;57(3):235–45.
[10] Rockinger O. Image sequence fusion using a shift-invariant wavelet transform. Proceedings of IEEE international conference on image processing, vol. 3. p. 288–91.
[11] Blum RS, Liu Z. Multi-sensor image fusion and its applications. CRC Press, Taylor & Francis Group; 2006.
[12] Goshtasby A, Nikolov S. Image fusion: advances in the state of the art. Inform Fusion 2007;8(2):114–8.
[13] Tang J. A contrast based image fusion technique in the DCT domain. Digit Signal Process 2004;14(3):218–26.
[14] Wallace GK. The JPEG still picture compression standard. Commun ACM 1991;34(4):30–44.
[15] Richardson IEG. Video codec design. John Wiley & Sons Ltd.; 2002.
[16] Wang Z, Bovik AC, Sheikh HR, Simoncelli EP. Image quality assessment: from error visibility to structural similarity. IEEE Trans Image Process 2004;13(4):600–12.
[17] Piella G, Heijmans H. A new quality metric for image fusion. Proceedings of international conference on image processing (ICIP), vol. 3. p. 173–6.
[18] Xydeas CS, Petrovic V. Objective image fusion performance measure. Electron Lett 2000;36(4):308–9.
[19] Available from: http://www.metapix.de/toolbox.htm.

Mohammad Bagher Akbari Haghighat received the B.Sc. and M.Sc. degrees in Electrical Engineering from University of Tabriz, Tabriz, Iran, in 2008 and 2010, respectively. Since 2008, he has been working as a research assistant in Laboratory of Image Processing and Computer Vision, University of Tabriz. His research interests are image processing, image fusion, computer vision, and information theory.

Ali Aghagolzadeh received the Ph.D. degree from Purdue University, West Lafayette, IN, USA, in 1991 in Electrical Engineering. He is currently a professor of Electrical Engineering in University of Tabriz, Tabriz, Iran, and in Babol University of Technology, Babol, Iran. His research interests include image processing, video coding and compression, information theory, and computer vision.

Hadi Seyedarabi received the Ph.D. degree in Electrical Engineering from University of Tabriz, Iran, in 2006. He is currently an assistant professor of Faculty of Electrical and Computer Engineering in University of Tabriz, Tabriz, Iran. His research interests are image processing, computer vision, Human–Computer Interaction, facial expression recognition, and facial animation.